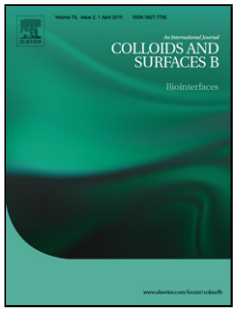

Title: Atomolar electrochemical detection of the BCR/ABL fusion gene based on an amplifying self-signal metal nanoparticle-conducting polymer hybrid composite

Author: Karen Y.P.S. Avelino Isaac Aaron Morales Norma Lucena-Silva Renan Garcia Gomes Celso P. de Melo Maria D.L. Oliveira César A.S. Andrade

PII: S0927-7765(16)30683-X
DOI: http://dx.doi.org/doi:10.1016/j.colsurfb.2016.09.029
Reference: COLSUB 8161

To appear in: *Colloids and Surfaces B: Biointerfaces*

Received date: 10-6-2016
Revised date: 5-9-2016
Accepted date: 21-9-2016

Please cite this article as: Karen Y.P.S.Avelino, Isaac Aaron Morales, Norma Lucena-Silva, Renan Garcia Gomes, Celso P.de Melo, Maria D.L.Oliveira, César A.S.Andrade, Atomolar electrochemical detection of the BCR/ABL fusion gene based on an amplifying self-signal metal nanoparticle-conducting polymer hybrid composite, Colloids and Surfaces B: Biointerfaces http://dx.doi.org/10.1016/j.colsurfb.2016.09.029

ATOMOLAR ELECTROCHEMICAL DETECTION OF THE BCR/ABL FUSION GENE BASED ON AN AMPLIFYING SELF-SIGNAL METAL NANOPARTICLE-CONDUCTING POLYMER HYBRID COMPOSITE

Karen Y.P.S. Avelino[1], Isaac Aaron Morales[2], Norma Lucena-Silva[3,4], Renan Garcia Gomes[3,4], Celso P. de Melo[5], Maria D.L. Oliveira[1,2], César A.S. Andrade[1,2*]

[1]Programa de Pós-Graduação em Bioquímica e Fisiologia, Universidade Federal de Pernambuco, 50670-901 Recife, PE, Brasil.

[2]Programa de Pós-Graduação em Inovação Terapêutica, Universidade Federal de Pernambuco, 50670-901 Recife, PE, Brasil.

[3]Centro de Pesquisas Aggeu Magalhães, Fundação Osvaldo Cruz (Fiocruz), 50670-420 Recife, PE, Brasil.

[4]Laboratório de Biologia Molecular, Departamento de Oncologia Pediátrica, Instituto de Medicina Integral Professor Fernando Figueira (IMIP), 50070-550 Recife, PE, Brasil.

[5]Departamento de Física, Universidade Federal de Pernambuco, 50670-901 Recife, PE, Brasil.

*To whom correspondence should be addressed.

C.A.S. Andrade, Departamento de Bioquímica, UFPE, 50670-901, Recife, PE, Brazil

Phone: +55-81-2126.8450; Fax: +55-81-2126.8547

E-mail: csrandrade@gmail.com

Graphical abstract

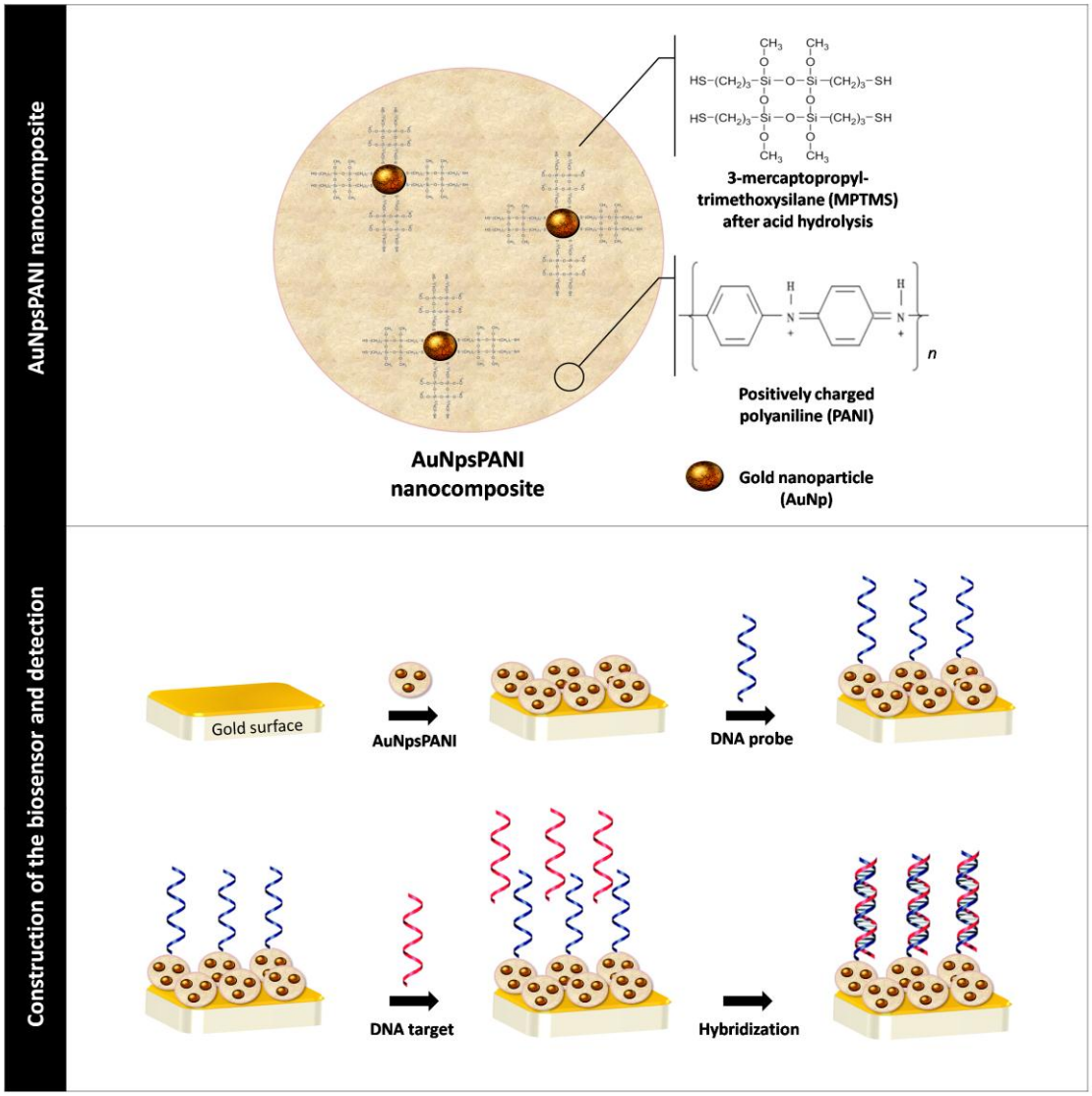

Highlights

- An electrochemical DNA sensor based on a nanostructured polyaniline-gold composite was developed.
- A simple and attractive tool for the molecular diagnosis of the BCR/ABL oncogene was obtained.
- The new hybrid sensing-platform displayed high specificity and selectivity.
- The device exhibited an excellent detection limit estimated to be as low as 69.4 aM

ABSTRACT

In the last ten years, conjugated polymers started to be used in the immobilization of nucleic acids via non-covalent interactions. In the present study, we describe the construction and use of an electrochemical DNA biosensor based on a nanostructured polyaniline-gold composite, specifically developed for the detection of the BCR/ABL chimeric oncogene. This chromosome translocation is used as a biomarker to confirm the clinical diagnosis of both chronic myelogenous leukemia (CML) and acute lymphocytic leukemia (ALL). The working principle of the biosensor rests on measuring the conductivity resulting from the non-covalent interactions between the hybrid nanocomposite and the DNA probe. The nanostructured platform exhibits a large surface area that enhances the conductivity. Positive cases, which result from the hybridization between DNA probe and targeted gene, induce changes in the amperometric current and in the charge transfer resistance (R_{CT}) responses. Atomic force microscopy (AFM) images showed changes in the genosensor surface after exposure to cDNA sample of patient with leukemia, evidencing the hybridization process. This new hybrid sensing-platform displayed high specificity and selectivity, and its detection limit is estimated to be as low as 69.4 aM. The biosensor showed excellent analytical performance for the detection of the BCR/ABL oncogene in clinical samples of patients with leukemia. Hence, this electrochemical sensor appears as a simple and attractive tool for the molecular diagnosis of the BCR/ABL oncogene even in early-stage cases of leukemia and for the monitoring of minimum levels of residual disease.

Keywords: BCR/ABL fusion gene; biosensor; electrochemistry; hybrid nanoparticles; leukemia.

1. Introduction

The occurrence of genetic disorders related to BCR/ABL chimeric oncogene represents a risk factor for the development of both CML in adults and ALL in children [1-4]. Prompt identification of BCR/ABL oncogene would enable an early diagnosis as well as the monitoring of the disease's remission [5, 6]. Currently, however, leukemia diagnosis is mainly performed in a qualitative manner and the concentration of the BCR/ABL fusion gene is not determined. While most patients are diagnosed by hematological examination [7], molecular methods to confirm clinical diagnosis include chromosome analysis [8], fluorescence *in situ* hybridization [9], flow cytometry [10] and quantitative real-time reverse-transcription polymerase chain reaction (qRT-PCR) [11]. We stress that in spite of their high sensitivity these techniques face major limitations for a more widespread application, which are associated to time-consuming protocols and high acquisition costs [12, 13]. Therefore, at present the development of a simple and effective molecular assay capable to detect the BCR/ABL fusion gene continues to be of great interest for allowing the effective implementation of adequate early-stage therapeutic strategies.

In recent years, significant advances in nanoscience and biotechnology have allowed a substantial improvement of the electrochemical DNA detection devices [14-16]. Covalent and non-covalent methods have been used in genosensors to immobilize small nucleic acid segments on numerous transducing materials [17]. However, the main challenge still relies on improving the ability of the transducer to detect small changes in the electrochemical properties of the sensor interface caused by the hybridization between the single-stranded DNA probes (ssDNA) and their complementary targets. For the most part, a secondary amplification of the signal needs

to be implemented in the form of electrochemical, chromatic, magnetic or metallic reporters [18-21].

New strategies are required to develop biosensors aiming to increase not only the immobilization efficiency of the probe but also the analytical performance of the transducer [22]. Within this perspective, conjugated polymers (CPs) are interesting materials to consider, since they are well known for their chemical stability, low cost polymerization and ability to be conformed into innumerable structures. In addition, the combination of their transport properties, electrical conductivity or rate of energy migration confers to them the possibility of an amplified sensitivity [23]. In special, the pH-dependent conductivity of polyaniline (PANI) allows this polymer to act as a direct electron mediator for the self-amplification of an electrochemical signal [24-26].

At the same time, metallic nanoparticles are also recognized as outstanding performers on electrochemical biosensor research [51-52]. Gold nanoparticles (AuNps) possess large surface free energy and a large area to volume ratio that provides for an enhanced electrochemically active surface. In fact, the size of the AuNps has a direct implication on their surface area. This intrinsic property of nanoscale materials is essential for obtaining biodevices with higher analytical performances [44-46]. Furthermore, AuNps can be used to promote the immobilization of biomolecules, while preserving their biological activity and directing the charge transfer between the biorecognition layer and the electrode surface [27-29].

In this manner, the use of organic-inorganic hybrid materials is emerging as an innovative alternative in biological sensor systems because of their unique synergy characteristics [26, 30-32]. For this reason, we propose that the association between AuNps and PANI can present promising features in the construction of selective and robust bio sensitive platforms [26, 32].

Herein, we describe the development of a label-free genosensor based on an AuNpsPANI hybrid composite for the electrochemical detection of the BRC/ABL fusion gene. The ssDNA used as capture probe was attached on the gold electrode modified with AuNpsPANI composite through electrostatic interactions. Cyclic voltammetry (CV), electrochemical impedance spectroscopy (EIS) and atomic force microscopy (AFM) were used to characterize the manufacturing process and to assess the performance of the biosensor.

2. Materials and methods

2.1. Materials

Tetrachloroauric acid ($HAuCl_4$) and 3-mercaptopropyl-trimethoxysilane (MPTMS) were purchased from Sigma Chemical (St. Louis, MO, USA). Aniline, potassium ferri- and ferrocyanide were obtained from VETEC (SP, Brazil). For the construction of the biosensor, the primer ALL (9;22) 5'-CGGTTGTCGTGTCCGAGG-3' was used as bio recognition probe. The chimeric transcript was obtained after the amplification of the BCR/ABL oncogene by using both the primer ALL and the primer CML (9;22) 5'-AGCTTCTCCCTGACATCCGTG-3'. Subsequently, the chimerical DNA fragment was subcloned in a pTA vector. The recombinant plasmid sequencing was performed using primers complementary to the plasmid backbone to confirm the subcloning of the chimeric BCR/ABL transcript (Supplementary information Fig. S1). The cDNA samples of patients with leukemia were obtained from the biorepository of the IMIP's Pediatric Oncology Service and kindly provided by Doctor Francisco Pedrosa. cDNA is obtained from the total RNA of patients using a random primer [54-55]. Therefore, the samples are free of contaminants. The gold standard for the

molecular monitoring of minimal residual disease in hematologic malignancies is the polymerase chain reaction that also requires genomic pre-amplification. The proposed molecular assay is performed in a lower number of steps for detection of the BCR/ABL fusion gene as compared to polymerase chain reaction (PCR). In addition, the proposed biosensor showed an exceptionally low detection limit and could become a very important tool for leukemia diagnosis and the monitoring of the minimal residual disease level.

2.2. Synthesis of AuNpsPANI hybrid composites

According to our early work [31], aniline (0.030 mol.L^{-1}), MPTMS (6.46×10^{-2} mol.L^{-1}), and $HAuCl_4$ (0.81 mmol.L^{-1}) were used to prepare the AuNpsPANI hybrid composite in ethanol solution under magnetic agitation (1100 rpm) at room temperature for 48 h [31]. After polymerization, the large agglomerates were removed from the sample by centrifugation at 12,000 RPM during 10 min. Finally, the pH of the medium was adjusted with an acidic solution (0.1 M HCl) to promote PANI protonation and MPTMS hydrolysis [32, 33]. The strategies for obtaining the sensor device and its biospecific recognition are schematically shown in Fig. 1. The initial step of the synthesis of the AuNpsPANI nanocomposite is based on the release of the ion H^+ from $HAuCl_4$ to the formation of anilinium cations ($PhNH_3^+$). The $[AuCl_4]^-$ acts as an oxidizing agent, promoting the oxidation of the $PhNH_3^+$ and giving rise to polyaniline. During the polymerization process occurs the release of electrons that reduce the $[AuCl_4]^-$ to form gold nanoparticles (AuNps). These AuNps are encapsulated by the polymer matrix. In addition, the 3-mercaptopropyl-trimethoxysilane (MPTMS) is used as a stabilizing agent to prevent the aggregation of the AuNps [31-33]. With this last

step, the sulfhydryl groups from MPTMS become ready to serve as a kind of molecular adhesive between the nanocomposite and the surface of the gold electrode.

2.3. Preparation of the biosensor and exposure to target DNA

Initially, the bare gold electrode (BGE, ϕ = 2 mm) was carefully polished with 0.05 µm α-Al_2O_3 paste and rigorously rinsed and sonicated in ultrapure water for 10 min. Subsequently, the electrode was electrochemically pretreated by CV scanning between 0.7 and -0.2V in $K_4[Fe(CN)_6]/K_3[Fe(CN)_6]$, until a typical clean gold CV curve was obtained. Next, BGE was dip coated into the 500 µL of AuNpsPANI solution diluted in ethanol in a 1:750 (v/v) ratio for 2 min at room temperature and rinsed with water to remove non-bonded nanocomposite particles. Subsequently, 2 µL of a at 25 pmol.μL^{-1}ALL biorecognition probe was dropped on the AuNpsPANI-modified electrode, which was incubated for 10 min. The selectivity and specificity of the genosensor were evaluated by using a recombinant plasmid containing the BCR/ABL fusion gene and a (nonspecific) plasmid with a non-complementary DNA sequence. We tested 0.0694, 0.694, 6.94, 69.4, 694 fM concentrations of recombinant plasmid containing the BCR/ABL fusion gene (positive control), while the concentration of the nonspecific plasmid used as negative control was 6.94 pM. Furthermore, the genosensor was tested with cDNA samples obtained from leukemia positive patients from IMIP. All diagnoses of chromosome translocation (in plasmidial and patient samples) were performed by dropping 2 µL of each sample solution that was kept on the genosensor surface for 15 min.

2.4. Electrochemical measurements

Electrochemical characterization was carried out on a Autolab PGSTAT 128N potentiostat/galvanostat interfaced with NOVA 1.8 software (Metrohm Autolab Inc., Netherlands). All measurements were performed on a three-electrode-configured electrochemical cell using a solution containing 10 mM $K_4[Fe(CN)_6]/K_3[Fe(CN)_6]$ (1:1) in PBS (10 mM, pH 7.4) as redox probe. The potential of CV measurements was swept between +0.7 V and -0.2 V at 50 mVs^{-1}scan rate. Impedance measurements were performed in the 100 mHz to 100 kHz frequency range under a +10 mV sine wave potential. The fabricated genosensor was used as working electrode, while platinum and Ag/AgCl electrodes (in 3M KCl) were used as counter and reference electrodes, respectively. All electrochemical measurements were repeated three times at room temperature inside a Faraday cage.

2.5 Atomic force microscopy measurements

The morphological characterization of the sensor before and after its interactions with the BCR/ABL fusion gene was performed using an atomic force microscope (SPM-9500J2; Shimadzu, Tokyo, Japan). Cantilevers with a silicon AFM probe (Multi 75AL, NCHR, 75 kHz resonant frequency, 3 $N.m^{-1}$ force constant) were used for the noncontact mode AFM in air at room temperature (approximately 25ºC). Lateral resolution was set to 512 × 512 pixels in a scan area of 5 × 5 µm. At least three areas in each sample were macroscopically separated for analysis. The AFM Gwyddion software was used to analyze the images (Necas et al., 2008).

3. Results

3.1. Morphological analyses

In Fig. 2 we show the changes in the morphology of the electrode surface as evaluated during the stepwise biosensor fabrication process. After evaporation of the solvent, AuNpsPANI nanocomposite particles arrange themselves into agglomerates with a height of 34.3 nm (Fig. 2A). However, the formation of a self-assembled monolayer (SAM) over the surface is favored due to the terminal thiol groups from MPTMS on AuNpsPANI nanocomposite. In Fig. 2B, we show that after the immobilization of the ALL primer the surface becomes uniform with an average height of 51 nm. In Fig. 2C, the morphology of the genosensor after exposure to cDNA sample extracted from whole blood of a positive leukemia patient is shown. As expected, a drastic change in the morphology of the sensor surface was observed, with the presence of peaks up to 82 nm. This result demonstrates the occurrence of specific interaction between the DNA probe and the BCR/ABL fusion gene present in patient sample with CML. On the other hand, non-significant changes in the morphology of the genosensor were observed after its exposure to a patient sample without CML (average height of 59 nm) (Fig. 2D). The height difference for non-complementary samples as compared to the AuNpsPANI-DNA probe can be attributed to a non-specific adsorption on the sensor surface [53].

3.2. Electrochemical characterization

The impedimetric responses shown in Fig. 3A were modelled according to a Randle's equivalent circuit (see inset of Fig. 3A) by use of the NOVA 1.8 software. The corresponding circuit includes (i) Rs, the ohmic resistance of the electrolyte solution, (ii) W_o, the Warburg impedance caused by the diffusion of ions from the bulk electrolyte to the electrode interface, (iii) C_{dl}, the double layer capacitance, and (iv) the charge transfer resistance R_{CT}, which is related to the microscopic processes occurring

close to the electrode surface. It is known that both distinct segments are associated to mass diffusion processes that predominantly control electron transfer. We found a smaller R_{CT} value (0.22kΩ) for BGE, in an indication that the charge transfer process is limited by electron diffusion. Compared to the initial BGE electrode, our results (a corresponding R_{CT} of 2.51 kΩ) indicate that the immobilization of the AuNpsPANI composite induces an increase in the interfacial resistivity of the electrode. This variation, which must be caused by a partial blockage of the charge transfer in the electrical double layer, suggests the formation of an AuNpsPANI monolayer. In addition, after the immobilization of the DNA probe on the AuNpsPANI-modified electrode, we noticed a significant increase (4.71 kΩ) in the R_{CT}. This result indicates that the negative charges of the tethered DNA probes effectively repel the redox agent, thus resulting in an additional increase in the R_{CT} value. Next, when the genosensor was exposed to a leukemia positive sample (be it plasmidial or patient cDNA) to promote hybridization, the increment on the number of negative charges causes the redox probe to be less prone to come nearby the genosensor surface, thus decreasing the overall electron transfer rate and consequently damping the intensity of the sensing signal. Nonetheless, the corresponding results can be still discussed in terms of the positive potential employed in the measurements. In this context, the applied DC potential attracts DNA strands to the surface of the electrode. However, the attractive forces are likely to be more effective over flexible ssDNA than over the stiffer double-stranded DNA (dsDNA) chains. Consequently, the physical barrier to the electrode surface will be more effective in the case when the hybridized complementary strand is substantially lengthier than the probe. Following this reasoning, when the genosensor is exposed to a sample (Section *3.4*) containing the whole genome of the patient, the observed increase in the R_{CT} value will not be necessarily caused solely by the amount of BCR/ABL

fusion gene copies found in the sample, since the length of the hybridized strand can also contribute to this result.

The electrochemical behavior of electrode was monitored at each step along the genosensor fabrication and the corresponding results are presented in Fig. 3B. The signal of the gold electrode shows a reversible voltammogram in the case of the redox probe. This behavior reveals that the electron transfer reaction is mainly a diffusion-controlled process. After the adsorption of the AuNpsPANI composite on the BGE surface, we noticed a decrease in the amperometric response. This was an expected behavior, since accordingly to the impedimetric results the immobilized nanocomposite should hinder the penetration of the redox probe through the freshly formed SAM. When compared to a BGE voltammogram, the electrode modified with AuNpsPANI and DNA probe exhibits a quasi-reversible behavior, with a considerable decrease in the oxidation/reduction signals and an increase in the separation of the peaks. Most likely, this low transfer rate of the redox couple in the sensor layer should depend on the degree of surface coating, an effect that we will study in more details in a following section.

Furthermore, DNA interaction can result in conformational alterations and changes in the electronic state (redox state) of the conductive polymer, as a planarization of the backbone and displacement of electrons [47, 48]. Consequently, the electrochemical properties of the polymer, such as electron transfer rate and its conductivity, can be altered. These events are triggered by the onset of electrostatic interactions, van der Waals forces and H-bonds between the DNA and polymeric chains [48]. Recent reports have suggested that the DNA can control the redox functions of PANI chains, generating a supra-molecular structure of two oppositely charged polyelectrolytes [49, 50]. These changes, which would occur predominantly in the outer

layers of the polymer in contact with the biomolecule, cause perturbations in the electrical double layer (such as changes in capacitance, conductance, resistance and impedance) that can be monitored by conventional electrochemical techniques [49].

3.3. Selectivity and sensitivity assays

In Fig. 4A we compare the cyclic voltammograms that were obtained when the genosensor was exposed to different concentrations of plasmidial DNA containing the BCR/ABL fusion gene (target DNA -0.0694, 0.694, 6.94, 69.4, 694 fM) and non-complementary plasmidial DNA (6.94 pM). After the biospecific interaction process, we observed a decrease in the redox peak currents and a reduction in the voltammetric areas. Our results are in accordance to earlier reports [34] that indicate that the hybridization process leads to a gradual reduction of the amperometric response. In this sense, a decrease on the electrochemical response is associated to a reduction on the electron flow rate through the biorecognition layer.

We can define the biodetection degree of the genosensor as the percentage of relative deviation of the anodic current variation (ΔI) between tested samples, which corresponds to

$$\Delta I(\%) = \frac{I_b - I_a}{I_a} . 100 \, , \qquad (1)$$

where I_b and I_a correspond to the anodic peak current before and after the hybridization process, respectively. In Table S1, we present the results of ΔI (%) for the AuNpsPANI-DNA probe genosensor, before and after exposure to different concentrations of the target DNA. We take notice of the fact that the gradual increase in the ΔI value correlates well with the rise on the target DNA concentration. After exposing the genosensor to the negative control, we observed a subtle change in the anodic peak current (ΔI = 6.85 %). Although insignificant when compared to the result obtained for

even the lower concentration of recombinant plasmid containing the BCR/ABL fusion gene (ΔI = 60.10 %), this result indicates that highly concentrated negative samples might produce a low but non-negligible response, probably as a consequence of the unspecific physical trapping of non-complementary strands.

In Fig. 4B we present the impedimetric behavior of the genosensor after its exposure to plasmidial DNA containing the BCR/ABL fusion gene and to non-complementary plasmidial DNA. We can observe that the EIS results are in agreement with the results obtained by CV.

The results obtained by modelling the data with basis on a Randle's circuit are shown in Table S2. It is convenient to evaluate the performance of the genosensor in terms of the relative variation of the R_{CT} (ΔR_{CT} (%)), which is defined as

$$\Delta R_{CT}(\%) = \frac{R_{CT(Genosensor-target\ DNA)} - R_{CT(Genosensor)}}{R_{CT(Genosensor)}}.100\ , \qquad (2)$$

where $R_{CT(Genosensor\text{-}target\ DNA)}$ is the measured value after the target DNA has hybridized with the probe, and $R_{CT(Genosensor)}$ corresponds to the initial response of the AuNpsPANI-DNA probe genosensor. In the inset of Fig. 4B, one can see that a linear relationship exists between ΔR_{CT} and the target DNA concentration, with perceptible changes in the ΔR_{CT} values being observed at the different values of the latter. From the impedance analysis, we estimated the lowest detection limit as 69.4 aM (41 DNA copies per µL), a more stringent threshold relative [OK??] to the sensibility range (10^{-8} to 10^{-15} mol.L^{-1}) found in earlier reports on methods for detecting the BCR/ABL fusion gene [5, 6, 35, 36]. The detection limit of the genosensor corresponds to lower concentration of the plasmidial sample containing the BCR/ABL fusion gene. The concentrations of 0.0694, 0.694, 6.94, 69.4, 694 fM were evaluated. The detection limit of the genosensor is 69.4 aM (or 0.0694 fM). In addition, in a demonstration of its robust specificity, a low ΔR_{CT}

was obtained during the interaction of the genosensor with a non-complementary plasmid.

3.4. Detection of the BRC/ABL fusion gene in patient samples

We treated the patient samples, which were obtained after informed consent, randomly and anonymously during the analysis. All samples were previously diagnosed by conventional PCR and ethidium bromide stained agarose gel electrophoresis (Fig. S2 in the Supplementary Information). In this manner, we can ensure the reliability of the results obtained from the proposed sensor system. In Fig. S2 we present the results of the electrophoresis for the PCR products. The positive control for the BCR/ABL fusion gene (CTR+) shows a light band in the gel at about 435bp. However, no bands were observed for the negative control (CTR-) samples. The A1 and B1 patient samples (cDNA), which correspond to CML positive diagnosis, show sharp bands in the gel, a fact coherent with the finding of the band in the positive control. The A2 sample, from a patient with negative residual disease, does not present any band related to the BCR/ABL fusion gene. Also, the B2 patient sample, which comes from a weakly positive residual disease case, exhibits a very low intensity brand, indicating a low expression of the BCR/ABL fusion gene. The glyceraldehyde-3-phosphate dehydrogenase (GAPDH) was used as an internal control for sample loading and in addition have allowed us to verify that the sample processing was efficient, discarding the possibility of its degradation. This constitutive gene is expressed at high levels in most tissues and cells independently of the adopted experimental conditions.

In Fig. 5A, we present the voltammetric response of the genosensor after exposure to cDNA samples of leukemia patients at different dilutions (1:1, 1:5, 1:10, 1:20 and 1:30). We noticed a decrease in the peak current values that were obtained

after the AuNpsPANI-DNA probe genosensor interact with the cDNA samples. The sensitivity of the genosensor to detect the BCR/ABL fusion gene in patient samples was monitored by measuring the variation of the anodic peak current (Table S1). In addition, we have verified that the ΔI (%) values decrease as the samples are progressively diluted (Supplementary information Fig. S3).

In Fig. 5B we present the EIS responses in the form of Nyquist plots. The incubation of the genosensor with patient cDNA samples resulted in an increase of the R_{CT} at the electrode/electrolyte interface, in a confirmation that the BCR/ABL fusion gene is present. In Table S2, we show the information obtained through the theoretical modeling of the EIS results. In addition, we present the degree of surface coating (Θ), a parameter used to evaluate the bioactivity of the sensor, which was calculated as

$$\theta = 1 - \frac{R_{CT(Genosensor)}}{R_{CT(Genosensor-cDNA\ sample)}} . \quad (3)$$

In this equation, $R_{CT(Genosensor)}$ is the charge transfer resistance of the AuNpsPANI-DNA probe genosensor and $R_{CT(Genosensor\text{-}cDNA\ sample)}$ is the corresponding value for the sensor after exposure to each sample. Knowledge of the Θ values allows the quantification of the percent coverage of the sensor surface after the biospecific recognition [16]. Naturally, these values are correlated to the number of hybridized DNA strands at the sensor surface. Hence, the study of Θ provides additional and complementary information about the biodetection process. In Fig. S4 we show the percentage of surface coverage after the interaction of the genosensor with the samples. These results confirmed the filling of the recognition sites by the BRC/ABL fusion gene, as a result of their hybridization with the cDNA samples.

From the bioanalytical studies previously presented it was possible to estimate the optimal dilution factor for performing the detection in clinical samples. It is probable that the less diluted samples (1:1 e 1:5) cause a nonspecific adsorption of the

oligonucleotides on the sensor surface due to the high concentration of interfering [???]. As demonstrated in Fig. S4, there was an exponential increase in the Θ values for the dilutions 1:1 and 1:5. For this reason, the dilution 1:10 was chosen as the most adequate for the implementation of electrochemical tests using actual leukemia patient samples.

In Fig. 5C we show the bioactivity of the genosensor after incubation with eight samples coming from different patients. According to the corresponding ΔR_{CT} values, we identify two groups of samples. The first (columns in red) is composed of CML positive samples, obtained in the diagnosis of cancer, while the group of columns in green is composed of CML negative samples, which were obtained from patients in the final stage of their treatment (i.e., with negative residual disease). As it can be verified, there is a large variation in the ΔR_{CT} values (from 161.14% to 297.73%) for the genosensor exposed to positive samples and an insignificant change for the case of negative samples (39.84% to 46.07%). Also, the electrochemical responses for the CML negative samples are very similar. This response profile can be attributed to the biorecognition of the ABL and BCR constitutive genes that can bind with the probe. In summary, the AuNpsPANI-DNA probe genosensor has shown an excellent specificity and the ability to discriminate between CML positive and negative samples. In addition, it has also demonstrated high sensitivity for the diagnosis of leukemia and monitoring of the level of minimal residual disease.

4. Discussion

We believe that the above results confirm that these AuNpsPANI based biosensors exhibit the necessary bioactivity, sensibility and specificity to be used as sensing platforms for actual leukemia patient samples. In addition, when compared to other BCR/ABL fusion gene sensors described in the literature [12, 37], our genosensor

demands a shorter preparation time while achieving an outstanding detection limit (Table 1).

The proposed nanostructured platform presents chemical stability and high surface area. The microenvironment created by the AuNpsPANI hybrid composite ensures a stable immobilization of DNA probes, with the maintenance of their conformational structure. In association with the electrochemical kinetics of the platform, these properties are valuable for the detection capability of a low concentration of the BCR/ABL fusion gene. To the best of our knowledge the detection limit of the proposed genosensor (69.4 aM) is the lowest concentration at which the BCR/ABL fusion gene was detected. Moreover, the detection process is fast, label-free and requires a small sample volume.

In fact, only 12 minutes are required to modify and immobilize the probe, and the label-free biodetection can be implemented within a total time of 15 minutes. These values should be compared to the estimated time involved in the construction of other sensor platforms, which varies from 30 minutes to 19 hours [5, 6, 12, 35, 36, 38-40]. Then, the construction time of our platform appears as the lowest reported in the literature. We attribute this difference to the chemisorption strategy adopted to structure our sensor platform. The principle of construction is based on the strong affinity between sulfur atoms of MPTMS (molecule present in the nanocomposite) and gold atoms of the electrode. Subsequently, DNA probe is electrostatically immobilized on the modified electrode for obtaining AuNpsPANI-DNA probe genosensor.

We emphasize that not all platforms consider the covalent immobilization of the DNA probe. At the same time, when used as active transducing elements in genosensors, materials such as carbon nanotubes, cerium dioxide nanoparticles,

chitosan [35], iron-platinum nanoparticles [40] and graphene sheets [6] usually demand the presence of a secondary signal amplifier or reporter.

In addition, while all biosensors must have as a minimal requirement a good detection capability, other properties should be considered for their clinical and commercial applicability, such as construction simplicity, fast response time and low cost. The molecular assay here described is performed in a lower number of steps for detection of the BCR/ABL fusion gene as compared to polymerase chain reaction (PCR), the gold standard method for the molecular monitoring of minimal residual disease in hematologic malignancies [56]. In addition, the proposed biosensor showed an exceptional detection limit and could become a very important tool for leukemia diagnosis and monitoring of the level of minimal residual disease.

5. Conclusions

We constructed an electrochemical DNA biosensor based on AuNpsPANI hybrid composite that exhibits high specificity and selectivity to detect the presence of the BCR/ABL fusion gene in leukemia patient samples. The voltammetric and impedimetric analyses were used not only to follow the process of preparation of these sensor systems, but also to test their biospecific recognition capability. These biosensors displayed a detection limit of 69.4 aM in the diagnosis of the presence of the BCR/ABL fusion gene in patient samples. In fact, we have showed that due to their sensitivity and analytical performance these AuNpsPANI-DNA probe systems can be used in an efficient for the diagnosis of leukemia and monitoring of minimal residual disease. Also, this label-free biodetection system can be built in a short time and at low cost. Therefore, we suggest that the biosensor here described appears as a promising

alternative tool for clinical research of the BCR/ABL chimeric oncogene, by allowing the diagnosis of early-stage cancer.

Acknowledgements

The authors are grateful for the support provided by the Brazilian National Council for Scientific and Technological Development (CNPq), Rede ELINOR de Nanobiotecnologia/CAPES, MCT/FINEP, PROPESQ/UFPE and FACEPE-PPSUS-APQ-0040-4.00/13. The authors are also grateful to Doctor Francisco Pedrosa for providing the cDNA samples stored in the biorepository of the Pediatric Oncology Service at the IMIP and Nucleus of Technology Platforms of the Research Center Aggeu Magalhães, Fiocruz-PE, Brazil, by the sequencing of recombinant transcripts.

Table Caption

Table 1. Comparison of the analytical performance of the AuNpsPANI biosensor with other electrochemical DNA biosensors developed to detect BCR/ABL fusion gene.

References	Sensor platform	Detection technique	Platform construction time	Electrochemical detection time	Detection limit
This Work	Gold surface /AuNpsPANI / DNA probe	CV and EIS	12 min	15 min	69.4×10^{-18} M
[5]	Glassy carbon surface / DNA probe with terminal amino group	DPV	-	35 min	5.9×10^{-8} M
[38]	Gold surface / DNA probe (thiolated hairpin locked nucleic acids)	CV, EIS and DPV	3 hours	~ 1 hour	1.2×10^{-10} M
[6]	Glassy carbon surface /graphene sheets / chitosan / PANI / AuNps / DNA probe	CV, EIS and DPV	~ 19 hours	~ 2.5 hours	2.11×10^{-12} M
[13]	ITO coated glass substrate / nanostructured composite of chitosan and cadmium-telluride quantum dots / DNA probe with terminal amino group	CV and DPV	~ 16.5 hours	1 min	2.56×10^{-12} M
[36]	Glassy carbon surface / DNA probe	CV, EIS and DPV	-	35 min	3×10^{-12} M
[35]	Glassy carbon surface / chitosan / cerium dioxide / multiwalled carbon nanotubes / AuNps / thiolated DNA probe	CV and DPV	~ 1.5 hours	55 min	5×10^{-13} M
[12]	Glassy carbon surface / sulfonic-terminated aminobenzenesulfonic acid / DNA probe (18-mer locked nucleic acids)	CV, EIS and *DPV	~ 30 min	~ 35 min	9.4×10^{-13} M
[41]	Gold surface / thiolated DNA probe (CdSeTe/CdS quantum dots tagging)	ASV	~ 13 hours	~ 18.5 hours	2×10^{-15} M
[40]	Carbon paste surface /FePt nanoparticles / electrochemically reduced graphene oxide/ DNA probe	EIS	-	-	2.6×10^{-15} M
[42]	Gold surface / thiolate DNA probe	CV and EIS	3 hours	1 hour	10×10^{-15} M
[43]	Indium-tin oxide (ITO) coated glass substrate / tri-n-octylphosphine oxide-capped cadmium selenide quantum dots / thiolated DNA probe	DPV	~ 30 min	2 min	10×10^{-15} M

Figure Captions

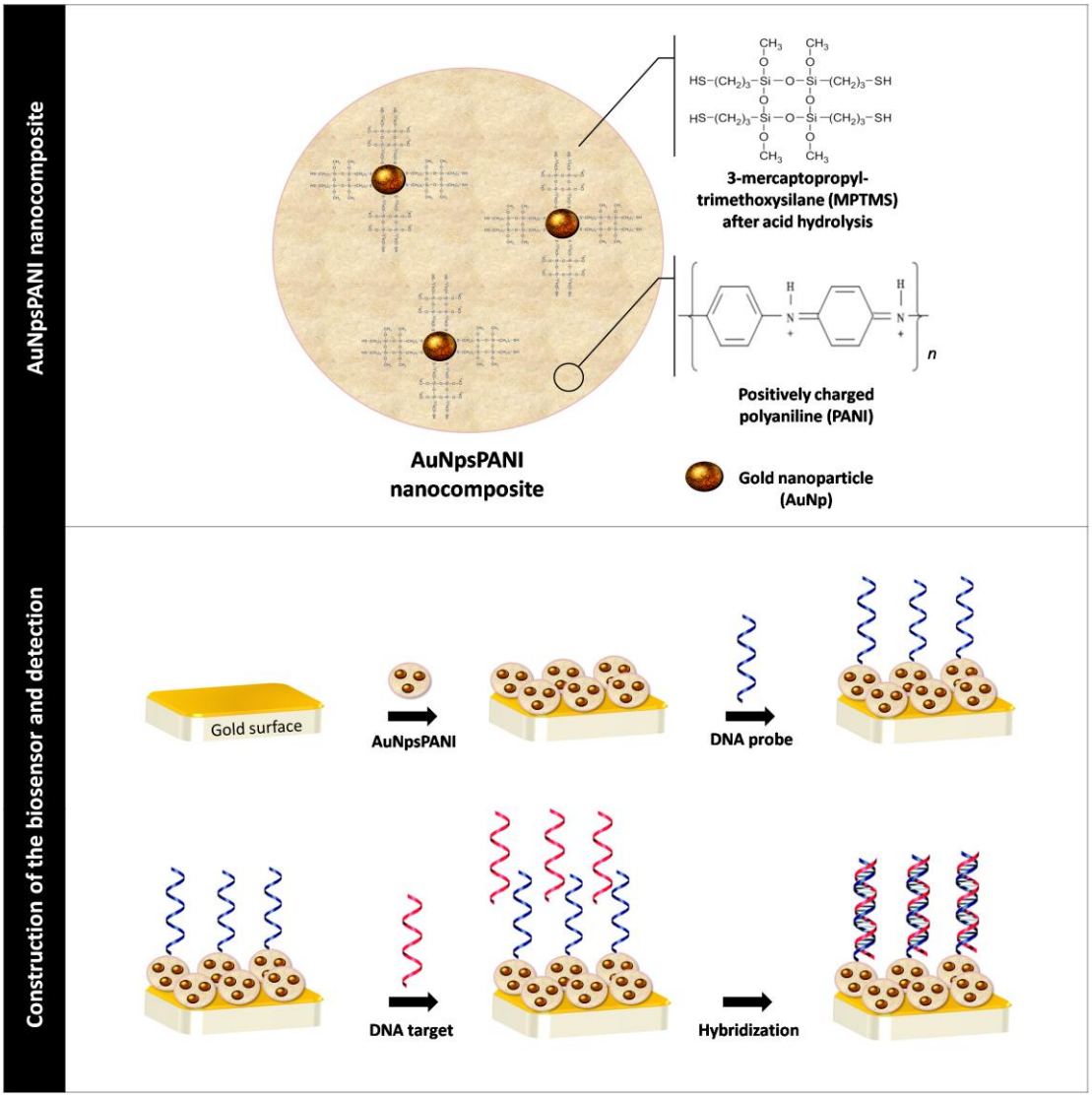

Figure 1. Schematic representation of the AuNpsPANI nanocomposite and construction of the biosensor.

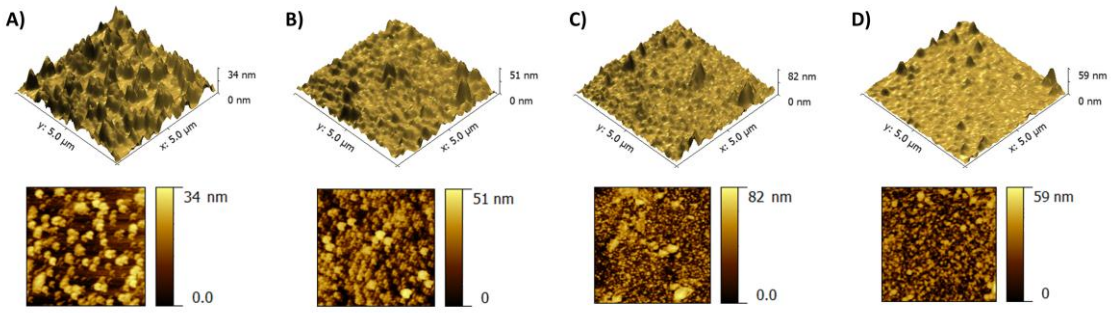

Figure 2. 3D and 2D AFM images of AuNpsPANI nanocomposite (A), AuNpsPANI-DNA probe (B), AuNpsPANI-DNA probe-CML positive patient sample (C) and AuNpsPANI-DNA probe-CML negative patient sample (D), with the corresponding cross section. Scan area of 5 µm × 5 µm.

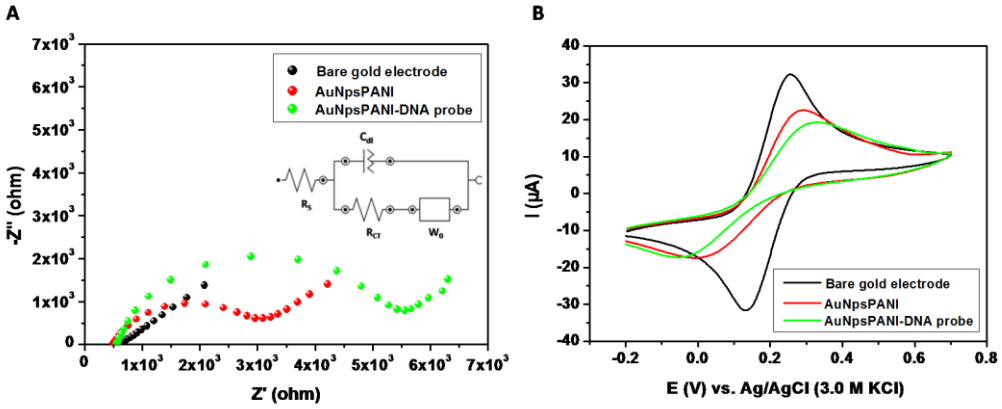

Figure 3. Nyquist plots (A) and cyclic voltammograms (B) for each step in the assembling of the genosensor. Inset: Equivalent circuit used to fit the impedance results.

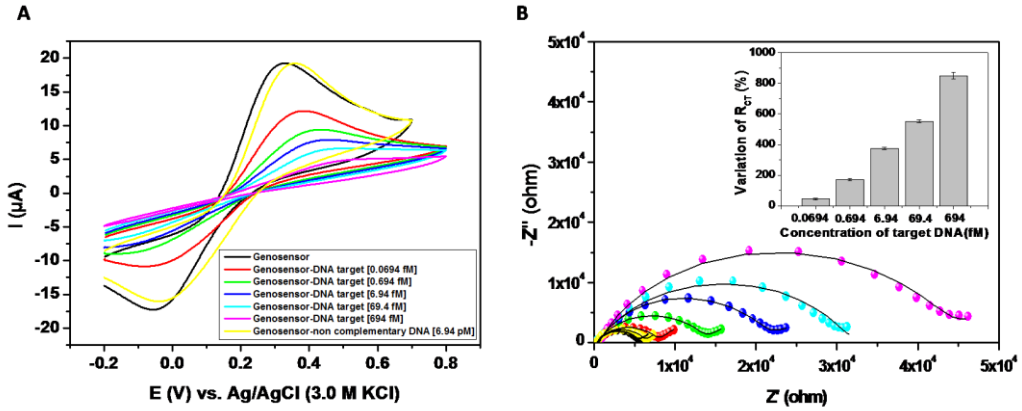

Figure 4. Cyclic voltammograms (A) and Nyquist plots (B) of the genosensor exposed to different concentrations of recombinant plasmid containing the BCR/ABL fusion gene (DNA target - 0.0694, 0.694, 6.94, 69.4, 694 fM) and nonspecific plasmid (negative control). Inset: ΔR_{CT} (%) of the genosensor after exposure to different concentrations of target DNA. Three replicates for each experimental condition were used. Experimental values are reported as the mean values ± their half-deviation (less than 3%).

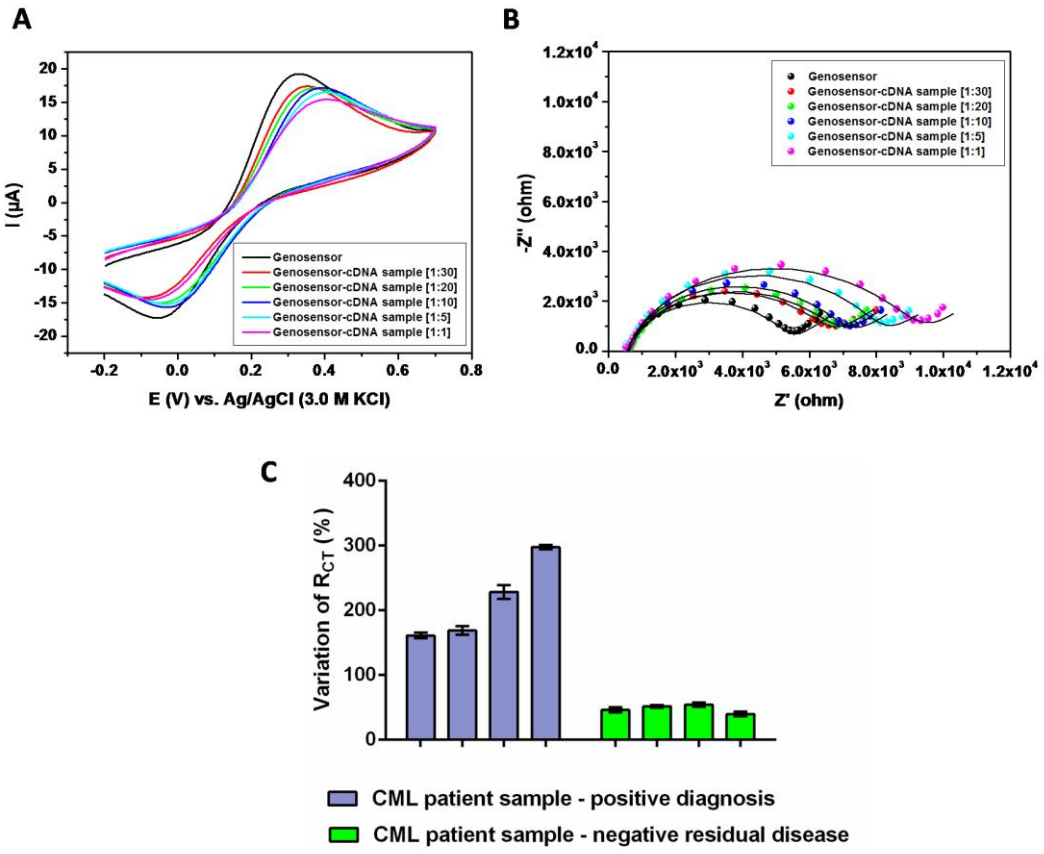

Figure 5. Cyclic voltammograms (A) and Nyquist plots (B) of the genosensor exposed to cDNA samples of leukemia patients at different dilutions (1:1, 1:5, 1:10, 1:20 and 1:30). Histogram showing the ΔR_{CT} (%) of the genosensor after exposure to CML positive and negative patient samples (C). Three replicates for each experimental condition were used. Experimental values are reported as the mean values ± their half-deviation (less than 3%).

References

[1] C. Cobaleda, N. Gutiérrez-Cianca, J. Pérez-Losada, T. Flores, R. García-Sanz, M. González, et al., A primitive hematopoietic cell is the target for the leukemic transformation in human Philadelphia-positive acute lymphoblastic leukemia2000.
[2] C.J. Harrison, Acute lymphoblastic leukaemia, Best Practice & Research Clinical Haematology, 14(2001) 593-607.
[3] C.G. Mullighan, C.B. Miller, I. Radtke, L.A. Phillips, J. Dalton, J. Ma, et al., BCR-ABL1 lymphoblastic leukaemia is characterized by the deletion of Ikaros, Nature, 453(2008) 110-4.
[4] A.S. Advani, A.M. Pendergast, Bcr–Abl variants: biological and clinical aspects, Leukemia Research, 26(2002) 713-20.
[5] X.-H. Lin, P. Wu, W. Chen, Y.-F. Zhang, X.-H. Xia, Electrochemical DNA biosensor for the detection of short DNA species of Chronic Myelogenous Leukemia by using methylene blue, Talanta, 72(2007) 468-71.
[6] L. Wang, E. Hua, M. Liang, C. Ma, Z. Liu, S. Sheng, et al., Graphene sheets, polyaniline and AuNPs based DNA sensor for electrochemical determination of BCR/ABL fusion gene with functional hairpin probe, Biosensors and Bioelectronics, 51(2014) 201-7.
[7] H. Parry, S. Damery, N. Mudondo, P. Hazlewood, T. McSkeane, S. Aung, et al., Primary Care Management of early stage Chronic Lymphocytic Leukaemia is safe and effective2015.
[8] S. Soverini, A. Hochhaus, F.E. Nicolini, F. Gruber, T. Lange, G. Saglio, et al., BCR-ABL kinase domain mutation analysis in chronic myeloid leukemia patients treated with tyrosine kinase inhibitors: recommendations from an expert panel on behalf of European LeukemiaNet2011.
[9] A.S. Corbin, A. Agarwal, M. Loriaux, J. Cortes, M.W. Deininger, B.J. Druker, Human chronic myeloid leukemia stem cells are insensitive to imatinib despite inhibition of BCR-ABL activity, The Journal of Clinical Investigation, 121(2011) 396-409.
[10] F. D'Alessio, P. Mirabelli, E. Mariotti, M. Raia, R. Di Noto, G. Fortunato, et al., Miniaturized flow cytometry-based BCR-ABL immunoassay in detecting leptomeningeal disease, Leukemia Research, 35(2011) 1290-3.
[11] A. Bennour, I. Ouahchi, M. Moez, M. Elloumi, A. Khelif, A. Saad, et al., Comprehensive analysis of BCR/ABL variants in chronic myeloid leukemia patients using multiplex RT-PCR, Clinical laboratory, 58(2011) 433-9.
[12] J. Chen, J. Zhang, K. Wang, X. Lin, L. Huang, G. Chen, Electrochemical Biosensor for Detection of BCR/ABL Fusion Gene Using Locked Nucleic Acids on 4-Aminobenzenesulfonic Acid-Modified Glassy Carbon Electrode, Analytical Chemistry, 80(2008) 8028-34.
[13] A. Sharma, C.M. Pandey, G. Sumana, U. Soni, S. Sapra, A.K. Srivastava, et al., Chitosan encapsulated quantum dots platform for leukemia detection, Biosensors and Bioelectronics, 38(2012) 107-13.
[14] C. Jianrong, M. Yuqing, H. Nongyue, W. Xiaohua, L. Sijiao, Nanotechnology and biosensors, Biotechnology Advances, 22(2004) 505-18.
[15] L. Sun, L. Yu, W. Shen, DNA nanotechnology and its applications in biomedical research, Journal of biomedical nanotechnology, 10(2014) 2350-70.
[16] D.M.N. Luna, K.Y.P.S. Avelino, M.T. Cordeiro, C.A.S. Andrade, M.D.L. Oliveira, Electrochemical immunosensor for dengue virus serotypes based on 4-mercaptobenzoic acid modified gold nanoparticles on self-assembled cysteine monolayers, Sensors and Actuators B: Chemical, 220(2015) 565-72.
[17] A. Sassolas, B.D. Leca-Bouvier, L.J. Blum, DNA Biosensors and Microarrays, Chemical Reviews, 108(2008) 109-39.
[18] S. Jampasa, W. Wonsawat, N. Rodthongkum, W. Siangproh, P. Yanatatsaneejit, T. Vilaivan, et al., Electrochemical detection of human papillomavirus DNA type 16 using a pyrrolidinyl peptide nucleic acid probe immobilized on screen-printed carbon electrodes, Biosensors and Bioelectronics, 54(2014) 428-34.

[19] L. Civit, A. Fragoso, C.K. O'Sullivan, Electrochemical biosensor for the multiplexed detection of human papillomavirus genes, Biosensors and Bioelectronics, 26(2010) 1684-7.
[20] N. Nasirizadeh, H.R. Zare, M.H. Pournaghi-Azar, M.S. Hejazi, Introduction of hematoxylin as an electroactive label for DNA biosensors and its employment in detection of target DNA sequence and single-base mismatch in human papilloma virus corresponding to oligonucleotide, Biosensors and Bioelectronics, 26(2011) 2638-44.
[21] S.X. Wang, G. Li, Advances in Giant Magnetoresistance Biosensors With Magnetic Nanoparticle Tags: Review and Outlook, Magnetics, IEEE Transactions on, 44(2008) 1687-702.
[22] S. Sagadevan, M. Periasamy, Recent trends in nanobiosensors and their applications-a review, Rev Adv Mater Sci, 36(2014) 62-9.
[23] D.T. McQuade, A.E. Pullen, T.M. Swager, Conjugated Polymer-Based Chemical Sensors, Chemical Reviews, 100(2000) 2537-74.
[24] Y. Cao, P. Smith, A.J. Heeger, Counter-ion induced processibility of conducting polyaniline and of conducting polyblends of polyaniline in bulk polymers, Synthetic Metals, 48(1992) 91-7.
[25] R.Y. Suckeveriene, E. Zelikman, G. Mechrez, M. Narkis, Literature review: Conducting carbon nanotube/polyaniline nanocomposites, Reviews in Chemical Engineering, 27(2011) 15-21.
[26] C. Liu, D. Jiang, G. Xiang, L. Liu, F. Liu, X. Pu, An electrochemical DNA biosensor for the detection of Mycobacterium tuberculosis, based on signal amplification of graphene and a gold nanoparticle-polyaniline nanocomposite, Analyst, 139(2014) 5460-5.
[27] S. Liu, D. Leech, H. Ju, Application of Colloidal Gold in Protein Immobilization, Electron Transfer, and Biosensing, Analytical Letters, 36(2003) 1-19.
[28] P. Yáñez-Sedeño, J.M. Pingarrón, Gold nanoparticle-based electrochemical biosensors, Anal Bioanal Chem, 382(2005) 884-6.
[29] J.M. Pingarrón, P. Yáñez-Sedeño, A. González-Cortés, Gold nanoparticle-based electrochemical biosensors, Electrochimica Acta, 53(2008) 5848-66.
[30] C. Sanchez, B. Julian, P. Belleville, M. Popall, Applications of hybrid organic-inorganic nanocomposites, Journal of Materials Chemistry, 15(2005) 3559-92.
[31] R.S. Santos, C.S. Andrade, C. dos Santos, C. de Melo, Visible luminescence in polyaniline/(gold nanoparticle) composites, J Nanopart Res, 15(2013) 1-11.
[32] K.Y.P.S. Avelino, C.A.S. Andrade, C.P. de Melo, M.L. Nogueira, M.T.S. Correia, L.C.B.B. Coelho, et al., Biosensor based on hybrid nanocomposite and CramoLL lectin for detection of dengue glycoproteins in real samples, Synthetic Metals, 194(2014) 102-8.
[33] H.P.O. Nascimento, M.D.L. Oliveira, C.P. de Melo, G.J.L. Silva, M.T. Cordeiro, C.A.S. Andrade, An impedimetric biosensor for detection of dengue serotype at picomolar concentration based on gold nanoparticles-polyaniline hybrid composites, Colloids and Surfaces B: Biointerfaces, 86(2011) 414-9.
[34] M.P. Costa, C.A.S. Andrade, R.A. Montenegro, F.L. Melo, M.D.L. Oliveira, Self-assembled monolayers of mercaptobenzoic acid and magnetite nanoparticles as an efficient support for development of tuberculosis genosensor, Journal of Colloid and Interface Science, 433(2014) 141-8.
[35] S. Li, L. Wang, Y. Li, X. Zhu, L. Zhong, L. Lu, et al., Electrochemical determination of BCR/ABL fusion gene based on in situ synthesized gold nanoparticles and cerium dioxide nanoparticles, Colloids and Surfaces B: Biointerfaces, 112(2013) 344-9.
[36] G.-X. Zhong, J.-X. Ye, F.-Q. Bai, F.-H. Fu, W. Chen, A.-L. Liu, et al., Electrochemical biosensor for detection of BCR/ABL fusion gene based on isorhamnetin as hybridization indicator, Sensors and Actuators B: Chemical, 204(2014) 326-32.
[37] A.A. Ensafi, M. Taei, H.R. Rahmani, T. Khayamian, Sensitive DNA impedance biosensor for detection of cancer, chronic lymphocytic leukemia, based on gold nanoparticles/gold modified electrode, Electrochimica Acta, 56(2011) 8176-83.

[38] L. Lin, X. Lin, J. Chen, W. Chen, M. He, Y. Chen, Electrochemical biosensor for detection of BCR/ABL fusion gene based on hairpin locked nucleic acids probe, Electrochemistry Communications, 11(2009) 1650-3.
[39] F. Wang, S. Hu, Electrochemical sensors based on metal and semiconductor nanoparticles, Microchim Acta, 165(2009) 1-22.
[40] J. Yang, W. Zhang, Indicator-free impedimetric detection of BCR/ABL fusion gene based on ordered FePt nanoparticle-decorated electrochemically reduced graphene oxide, J Solid State Electrochem, 18(2014) 2863-8.
[41] L. Hu, T. Tan, G. Chen, K. Zhang, J.-J. Zhu, Ultrasensitive electrochemical detection of BCR/ABL fusion gene fragment based on polymerase assisted multiplication coupling with quantum dot tagging, Electrochemistry Communications, 35(2013) 104-7.
[42] K. Wang, J. Chen, J. Chen, A. Liu, G. Li, H. Luo, et al., A Sandwich-Type Electrochemical Biosensor for Detection of BCR/ABL Fusion Gene Using Locked Nucleic Acids on Gold Electrode, Electroanalysis, 21(2009) 1159-66.
[43] A. Sharma, C.M. Pandey, Z. Matharu, U. Soni, S. Sapra, G. Sumana, et al., Nanopatterned Cadmium Selenide Langmuir–Blodgett Platform for Leukemia Detection, Analytical Chemistry, 84(2012) 3082-9.
[44] A. Bonanni; M. Pumera; Y. Miyahara. Influence of gold nanoparticle size (2–50 nm) upon its electrochemical behavior: an electrochemical impedance spectroscopic and voltammetric study. Physical Chemistry Chemical Physics, 13 (2011) 4980-6.
[45] S. Chen; R.S. Ingram; M.J. Hostetler; J.J. Pietron; R.W. Murray; T.G. Schaaff; J.T. Khoury; M.M. Alvarez; R.L. Whetten. Gold nanoelectrodes of varied size: transition to molecule-like charging, 280(1998), 2098-101.
[46] N. Nath; A. Chilkoti. Label-free biosensing by surface plasmon resonance of nanoparticles on glass: optimization of nanoparticle size. Analytical Chemistry, 76(2004) 5370-78.
[47] U. Lange; N.V. Roznyatovskaya; V.M. Mirsky. Conducting polymers in chemical sensors and arrays. Analytica chimica acta, 614(2008) 1-26.
[48] T. Ohtake; H. Tanaka. Redox-induced actuation in macromolecular and self-assembled systems. Polymer Journal, (2015).
[49] K. Arora; N. Prabhakar; S. Chand; B.D. Malhotra. Ultrasensitive DNA hybridization biosensor based on polyaniline. Biosensors and Bioelectronics, 23(2007), 613-20.
[50] Y. Xiao; A.B. Kharitonov; F. Patolsky; Y. Weizmann; I. Willner. Electrocatalytic intercalator-induced winding of double-stranded DNA with polyaniline. Chemical Communications, 13(2003), 1540-1.
[51] X. Luo; A. Morrin; A.J. Killard; M.R. Smyth. Application of nanoparticles in electrochemical sensors and biosensors. Electroanalysis,18(2006), 319-26.
[52] P.D. Howes; R. Chandrawati; M.M. Stevens. Colloidal nanoparticles as advanced biological sensors. Science, 346(2014.), 1247390.
[53] J. Wang; G. Rivas; J.R. Fernandes; J.L.L. Paz; M. Jiang; R. Waymire. Indicator-free electrochemical DNA hybridization biosensor. Analytica chimica acta, 375(1998), 197-203.
[54] E. Beillard; N. Pallisgaard; V.H.J. Van der Velden; W. Bi; R. Dee; E. van der Schoot; E. Delabesse; E. Macintyre; E. Gottardi; G. Saglio; F. Watzinger; T. Lion; J.J.M. van Dongen; P. Hokland; J. Gabert. Evaluation of candidate control genes for diagnosis and residual disease detection in leukemic patients using 'real-time'quantitative reverse-transcriptase polymerase chain reaction (RQ-PCR) – a Europe against cancer program. Leukemia, 17(2003), 2474-86.
[55] J. Gabert; E. Beillard; V.H.J. Van der Velden; W. Bi; D. Grimwade; N. Pallisgaard; G. Barbany; G. Cazzaniga; J.M. Cayuela; H. Cave; F. Pane; J.L.E. Aerts; D. De Micheli; X. Thirion; V. Pradel; M. González; S. Viehmann; M. Malec; G. Saglio; J.J.M. van Dongen. Standardization and quality control studies of 'real-time'quantitative reverse transcriptase polymerase chain reaction of fusion gene transcripts for residual disease detection in leukemia – a Europe Against Cancer Program. Leukemia, 17(2003), 2318-57.

[56] R. Mir; I. Ahmad; J. Javid; M. Zuberi; P. Yadav; R. Shazia; M. Masroor; S. Guru; P.C. Ray; N. Gupta; A. Saxena. Simple multiplex RT-PCR for identifying common fusion BCR-ABL transcript types and evaluation of molecular response of the a2b2 and a2b3 transcripts to Imatinib resistance in north Indian chronic myeloid leukemia patients. Indian Journal of Cancer, 52(2015), 314-8.

Table 1. Comparison of the analytical performance of the AuNpsPANI biosensor with other electrochemical DNA biosensors developed to detect BCR/ABL fusion gene.

References	Sensor platform	Detection technique	Platform construction time	Electrochemical detection time	Detection limit
This Work	Gold surface /AuNpsPANI / DNA probe	CV and EIS	12 min	15 min	69.4×10^{-18} M
(Lin et al. 2007)	Glassy carbon surface / DNA probe with terminal amino group	DPV	-	35 min	5.9×10^{-8} M
(Lin et al. 2009)	Gold surface / DNA probe (thiolated hairpin locked nucleic acids)	CV, EIS and DPV	3 hours	~ 1 hour	1.2×10^{-10} M
(Wang et al. 2014)	Glassy carbon surface /graphene sheets / chitosan / PANI / AuNps / DNA probe	CV, EIS and DPV	~ 19 hours	~ 2.5 hours	2.11×10^{-12} M
(Sharma et al. 2012)	ITO coated glass substrate / nanostructured composite of chitosan and cadmium-telluride quantum dots / DNA probe with terminal amino group	CV and DPV	~ 16.5 hours	1 min	2.56×10^{-12} M
(Zhong et al. 2014)	Glassy carbon surface / DNA probe	CV, EIS and DPV	-	35 min	3×10^{-12} M
(Li et al. 2013)	Glassy carbon surface / chitosan / cerium dioxide / multiwalled carbon nanotubes / AuNps / thiolate DNA probe	CV and DPV	~ 1.5 hours	55 min	5×10^{-13} M
(Chen et al. 2008)	Glassy carbon surface / sulfonic-terminated aminobenzenesulfonic acid / DNA probe (18-mer locked nucleic acids)	CV, EIS and *DPV	~ 30 min	~ 35 min	9.4×10^{-13} M
(Hu et al. 2013)	Gold surface / thiolate DNA probe (CdSeTe/CdS quantum dots tagging)	ASV	~ 13 hours	~ 18.5 hours	2×10^{-15} M
(Yang and Zhang 2014)	Carbon paste surface /FePt nanoparticles / electrochemically reduced graphene oxide/ DNA probe	EIS	-	-	2.6×10^{-15} M
(Wang et al. 2009)	Gold surface / thiolate DNA probe	CV and EIS	3 hours	1 hour	10×10^{-15} M
(Sharma et al. 2012a)	Indium-tin oxide (ITO) coated glass substrate / tri-n-octylphosphine oxide-capped cadmium selenide quantum dots / thiolate DNA probe	DPV	~ 30 min	2 min	10×10^{-15} M